Propagation properties of partially coherent Hermite–Gaussian beams through non-Kolmogorov turbulence*

He Xue-Mei(何雪梅) and Lü Bai-Da(吕百达)†

Institute of Laser Physics and Chemistry, Sichuan University, Chengdu 610064, *China*

(Received 16 January 2011; revised manuscript received 26 April 2011)

The propagation properties of partially coherent Hermite–Gaussian beams through non-Kolmogorov atmospheric turbulence are studied. The effects of non-Kolmogorov turbulence and beam nonparaxiality on the average intensity evolution and the beam-width spreading are stressed. It is found that the evolution of the average intensity distribution and the beam-width spreading depends on the generalized exponent factor, namely, on the non-Kolmogorov turbulence strength for the paraxial case. For the non-paraxial case the effect of the turbulence is negligible, while the beam-width spreading becomes very large. The analytical results are illustrated numerically and interpreted physically.

Keywords: non-Kolmogorov turbulence, partially coherent paraxial and non-paraxial Hermite–Gaussian beams, propagation

PACS: 42.68.Ay, 42.68.Bz, 42.25.Dd, 42.25.Fx **DOI:** 10.1088/1674-1056/20/9/094210

1. Introduction

Beam propagation through atmospheric turbulence has been extensively studied owing to its importance in basic science and attractive applications in optical communications and remote sensing.[1−8] It is believed that the use of spatial partially coherent beams can improve the performance of free-space communications, because partially coherent beams are less sensitive to the effects of turbulence than fully coherent ones.[9−14] The Kolmogorov power spectrum of refractive index fluctuation has been widely used for a long time for studying optical and radio wave propagation through the atmosphere. However, some experimental results show deviations from the predictions of the Kolmogorov model.[15−17] Recently, Toselli *et al.*[18,19] analysed the angle of arrival fluctuation and the optical system performance of a free-space laser beam propagating through the atmosphere by introducing a non-Kolmogorov model, in which a generalized exponent factor was used to replace the standard exponent value 11/3 in the Kolmogorov model. The propagation of the Gaussian–Schell model (GSM) and the cosh-Gaussian beams through non-Kolmogorov turbulence was illustrated by Wu *et al.*[20] and Chu *et al.*,[21] respectively, by using different turbulence models.

The motivation of this paper is to study the effect of non-Kolmogorov turbulence on the propagation properties of partially coherent Hermite–Gaussian (H–G) beams. The present paper is organized as follows. In Section 2, the analytical expression for the average intensity of the partially coherent H-G beam propagating through non-Kolmogorov turbulence is derived based on the extended Huygens–Fresnel principle and the non-Kolmogorov power spectrum introduced by Toselli *et al.*,[18] and is used to analyse the evolution of the average intensity distribution in non-Kolmogorov turbulence. In Section 3, the beam-width spreadings of the partially coherent paraxial and nonparaxial H–G beams are studied. Finally, some conclusions drawn from the present study are presented in Section 4.

2. Average intensity of partially coherent H–G beams in non-Kolmogorov turbulence

The electric field of H–G beams in the source plane $z = 0$ is written as[22]

*Project supported by the National Natural Science Foundation of China (Grant No. 10874125).

†Corresponding author. E-mail: baidalu0@tom.com

© 2011 Chinese Physical Society and IOP Publishing Ltd

$$U(\boldsymbol{\rho}, z=0) = \mathrm{H}_m\left(\frac{\sqrt{2}}{w_0}\rho_x\right)\mathrm{H}_n\left(\frac{\sqrt{2}}{w_0}\rho_y\right) \times \exp\left(-\frac{\rho_x^2+\rho_y^2}{w_0^2}\right), \quad (1)$$

where w_0 denotes the waist width of the corresponding Gaussian beam, $\boldsymbol{\rho} = (\rho_x,\ \rho_y)$ is the two-dimensional position vector, H_j denotes the Hermite polynomial of the j-th order ($j = m,\ n$) and an unimportant amplitude factor has been omitted.

Introducing the Schell-model correlator, the cross-spectral density of the partially coherent H–G beams in the plane $z = 0$ is expressed as[23]

$$W_0\left(\boldsymbol{\rho}_1, \boldsymbol{\rho}_2, 0\right) = \mathrm{H}_m\left(\frac{\sqrt{2}}{w_0}\rho_{1x}\right)\mathrm{H}_n\left(\frac{\sqrt{2}}{w_0}\rho_{1y}\right)\mathrm{H}_m\left(\frac{\sqrt{2}}{w_0}\rho_{2x}\right)\mathrm{H}_n\left(\frac{\sqrt{2}}{w_0}\rho_{2y}\right) \times \exp\left(-\frac{\boldsymbol{\rho}_1^2+\boldsymbol{\rho}_2^2}{w_0^2}\right)\exp\left[-\frac{(\boldsymbol{\rho}_1-\boldsymbol{\rho}_2)^2}{2\sigma_0^2}\right], \quad (2)$$

where σ_0 is the correlation length, and $\boldsymbol{\rho}_i = (\rho_{ix},\ \rho_{iy})$ ($i = 1,\ 2$, unless otherwise stated).

As shown in Ref. [24], based on the Rayleigh–Sommerfeld diffraction integral, the extended Huygens–Fresnel principle can be derived, which is generally applicable to both nonparaxial and paraxial cases and is given by

$$W(\boldsymbol{\rho'}_1, \boldsymbol{\rho'}_2, z) = \frac{z^2}{4\pi^2}\iint \mathrm{d}^2\rho_1 \iint \mathrm{d}^2\rho_2 W_0(\boldsymbol{\rho}_1, \boldsymbol{\rho}_2, 0)\frac{\exp[\mathrm{i}k(R_2-R_1)]}{R_1^3 R_2^3} \times(\mathrm{i}kR_2-1)(-1-\mathrm{i}kR_1)\langle\exp[\psi^*(\boldsymbol{\rho'}_1, \boldsymbol{\rho}_1)+\psi(\boldsymbol{\rho'}_2, \boldsymbol{\rho}_2)]\rangle, \quad (3)$$

where $\boldsymbol{\rho}'_i = (\rho_{ix},\ \rho_{iy})$ represents the two-dimensional position vector in the z plane, k denotes the wave number related to wavelength λ by $k = 2\pi/\lambda$, symbol * denotes the complex conjugate and

$$R_i = [(\rho'_{ix}-\rho_{ix})^2 + (\rho'_{iy}-\rho_{iy})^2 + z^2]^{1/2}. \quad (4)$$

The $\psi(\boldsymbol{\rho}'_i, \boldsymbol{\rho}_i)$ represents the random part of the complex phase of the spherical wave due to the existence of the turbulence, whose average over the ensemble of the turbulence medium reads[1,10]

$$\begin{aligned}
&\langle\exp[\psi^*(\boldsymbol{\rho'}_1, \boldsymbol{\rho}_1)+\psi(\boldsymbol{\rho'}_2, \boldsymbol{\rho}_2)]\rangle \\
&= \exp\left\{-4\pi^2k^2z\int_0^1\int_0^\infty \mathrm{d}\kappa\mathrm{d}\xi\kappa\Phi_n(\kappa,\alpha)[1-\mathrm{J}_0(\kappa\,|(1-\xi)(\boldsymbol{\rho'}_1-\boldsymbol{\rho'}_2)+\xi(\boldsymbol{\rho}_1-\boldsymbol{\rho}_2)|)]\right\} \\
&= \exp\left\{-\frac{\pi^2k^2z}{3}\int_0^\infty \kappa^3\Phi_n(\kappa,\alpha)\mathrm{d}\kappa[(\boldsymbol{\rho'}_1-\boldsymbol{\rho}'_2)^2+(\boldsymbol{\rho'}_1-\boldsymbol{\rho'}_2)(\boldsymbol{\rho}_1-\boldsymbol{\rho}_2)+(\boldsymbol{\rho}_1-\boldsymbol{\rho}_2)^2]\right\} \\
&= \exp\left\{-T(\alpha,z)[(\boldsymbol{\rho'}_1-\boldsymbol{\rho'}_2)^2+(\boldsymbol{\rho'}_1-\boldsymbol{\rho'}_2)(\boldsymbol{\rho}_1-\boldsymbol{\rho}_2)+(\boldsymbol{\rho}_1-\boldsymbol{\rho}_2)^2]\right\},
\end{aligned} \quad (5)$$

with J_0 being the Bessel function of the first kind and zero order and

$$T(\alpha,z) = \frac{\pi^2k^2z}{3}\int_0^\infty \kappa^3\Phi_n(\kappa,\alpha)\mathrm{d}\kappa. \quad (6)$$

The $\Phi_n(\kappa,\alpha)$ is the spatial power spectrum of the refractive-index fluctuation of the turbulence and for the non-Kolmogorov turbulence introduced by Toselli *et al.*[18] is given by

$$\Phi_n(\kappa,\alpha) = A(\alpha)\tilde{C}_n^2\frac{\exp(-\kappa^2/\kappa_m^2)}{(\kappa^2+\kappa_0^2)^{\alpha/2}}, \quad (0\le\kappa<\infty,\quad 3<\alpha<4), \quad (7)$$

$$A(\alpha) = \frac{1}{4\pi^2}\Gamma(\alpha-1)\cos\left(\frac{\alpha\pi}{2}\right), \quad (8)$$

$$\kappa_0 = \frac{2\pi}{L_0}, \quad (9)$$

$$\kappa_m = \frac{c(\alpha)}{l_0}, \quad (10)$$

$$c(\alpha) = \left[\Gamma\left(\frac{5-\alpha}{2}\right)A(\alpha)\frac{2\pi}{3}\right]^{1/(\alpha-5)}, \quad (11)$$

where $\Gamma(x)$ is the Gamma function, L_0 and l_0 are the outer and the inner scales of the atmospheric turbulence, respectively, and $\tilde{C}_n^2$ is the generalized structure constant. For $\alpha = 11/3$, $L_0 = \infty$, and $l_0 = 0$, we have $A(11/3) = 0.033$, $\tilde{C}_n^2 = C_n^2$ and the power spectrum $\Phi_n(\kappa, 11/3) = 0.033C_n^2\kappa^{-11/3}$, which has reduced to the ideal Kolmogorov power spectrum. It can be seen that $T(\alpha,z)$ describes the strength of the turbulence, namely, the larger $T(\alpha,z)$ corresponds to the stronger turbulence.

From Eqs. (6) and (7), we have

$$T(\alpha,z)=\frac{\pi^2k^2z}{6(\alpha-2)}A(\alpha)\tilde{C}_n^2\left\{-2\kappa_0^{(4-\alpha)}+\exp\left(\frac{\kappa_0^2}{\kappa_m^2}\right)\kappa_m^{(2-\alpha)}[(\alpha-2)\kappa_m^2+2\kappa_0^2]\Gamma\left(2-\frac{\alpha}{2},\frac{\kappa_0^2}{\kappa_m^2}\right)\right\}. \tag{12}$$

Under condition $R_i \gg \lambda$, equation (3) reduces to

$$W(\boldsymbol{\rho}_1',\boldsymbol{\rho}_2',z)=\frac{z^2}{\lambda^2}\iint \mathrm{d}^2\rho_1\iint \mathrm{d}^2\rho_2 W_0(\boldsymbol{\rho}_1,\boldsymbol{\rho}_2,0)\frac{\exp[\mathrm{i}k(R_2-R_1)]}{R_1^2R_2^2}\times\langle\exp[\psi^*(\boldsymbol{\rho}_1',\boldsymbol{\rho}_1)+\psi(\boldsymbol{\rho}_2',\boldsymbol{\rho}_2)]\rangle. \tag{13}$$

Substituting[25,26]

$$R_i\approx r_i+\frac{\rho_{ix}^2+\rho_{iy}^2-2\rho'_{ix}\rho_{ix}-2\rho'_{iy}\rho_{iy}}{2r_i} \tag{14}$$

into Eq. (13), we obtain

$$\begin{aligned}W(\boldsymbol{\rho}_1',\boldsymbol{\rho}_2',z)=&\frac{z^2}{\lambda^2r_1^2r_2^2}\exp[\mathrm{i}k(r_2-r_1)]\iint \mathrm{d}^2\rho_1\iint \mathrm{d}^2\rho_2 W_0(\boldsymbol{\rho}_1,\boldsymbol{\rho}_2,0)\\&\times\exp\left[\frac{\mathrm{i}k}{2r_2}(\rho_{2x}^2+\rho_{2y}^2-2\rho'_{2x}\rho_{2x}-2\rho'_{2y}\rho_{2y})-\frac{\mathrm{i}k}{2r_1}(\rho_{1x}^2+\rho_{1y}^2-2\rho'_{1x}\rho_{1x}-2\rho'_{1y}\rho_{1y})\right]\\&\times\langle\exp[\psi^*(\boldsymbol{\rho}_1',\boldsymbol{\rho}_1)+\psi(\boldsymbol{\rho}_2',\boldsymbol{\rho}_2)]\rangle.\end{aligned} \tag{15}$$

with

$$r_i=(\rho'^2_{ix}+\rho'^2_{iy}+z^2)^{1/2}. \tag{16}$$

By inserting $\boldsymbol{\rho}_1'=\boldsymbol{\rho}_2'=\boldsymbol{\rho}'$ and $r_1=r_2=r$ into Eq. (15), the average intensity of the partially coherent H–G beams propagating through the non-Kolmogorov turbulence is expressed as

$$\begin{aligned}I(\boldsymbol{\rho}',z)=&\frac{z^2}{\lambda^2r^4}\iint \mathrm{d}^2\rho_1\iint \mathrm{d}^2\rho_2 W_0(\boldsymbol{\rho}_1,\boldsymbol{\rho}_2,0)\exp\left[\frac{\mathrm{i}k}{2r}(\rho_2^2-\rho_1^2)\right]\\&\times\exp\left[\frac{\mathrm{i}k}{r}\boldsymbol{\rho}'(\boldsymbol{\rho}_1-\boldsymbol{\rho}_2)\right]\exp[-T(\alpha,z)(\boldsymbol{\rho}_1-\boldsymbol{\rho}_2)].\end{aligned} \tag{17}$$

Introducing $\boldsymbol{u}=(\boldsymbol{\rho}_1+\boldsymbol{\rho}_2)/2$ and $\boldsymbol{v}=\boldsymbol{\rho}_1-\boldsymbol{\rho}_2$ and substituting Eq. (2) into Eq. (17) yield

$$\begin{aligned}I(\boldsymbol{\rho}',z)=&\frac{z^2}{\lambda^2r^4}\iint \mathrm{d}^2u\iint \mathrm{d}^2v\mathrm{H}_m\left[\frac{\sqrt{2}}{w_0}\left(u_x+\frac{v_x}{2}\right)\right]\mathrm{H}_n\left[\frac{\sqrt{2}}{w_0}\left(u_y+\frac{v_y}{2}\right)\right]\mathrm{H}_m\left[\frac{\sqrt{2}}{w_0}\left(u_x-\frac{v_x}{2}\right)\right]\\&\times\mathrm{H}_n\left[\frac{\sqrt{2}}{w_0}\left(u_y-\frac{v_y}{2}\right)\right]\exp\left(-\frac{2u^2}{w_0^2}\right)\exp(-\varepsilon v^2)\exp\left(-\frac{\mathrm{i}k}{r}\boldsymbol{u}\boldsymbol{v}\right)\exp\left(\frac{\mathrm{i}k}{r}\boldsymbol{\rho}'\boldsymbol{v}\right),\end{aligned} \tag{18}$$

where

$$\varepsilon=\frac{1}{2w_0^2}+\frac{1}{2\sigma_0^2}+T(\alpha,z). \tag{19}$$

Recalling the integral formula[27]

$$\mathrm{L}_n^0(x)=\sum_{m=0}^{n}(-1)^m\binom{n}{n-m}\frac{x^m}{m!}, \tag{20}$$

with L_m^{n-m} being the Laguerre polynomial of orders m and $n-m$, tedious but straightforward diffractive integral calculations deliver

$$\begin{aligned}&I(\rho'_x,\rho'_y,z)\\=&\frac{\pi^2w_0^2z^2}{2\lambda^2r^4B}\exp\left[-\frac{k^2}{4r^2B}(\rho'^2_x+\rho'^2_y)\right]\times 2^{n+m}m!n!\\&\times\sum_{h=0}^{m}(-1)^h\binom{m}{m-h}\frac{a^h}{h!}(2h)!(\frac{\mathrm{i}k\rho'_x}{2Br})^{2h}\\&\times\sum_{l=0}^{h}\frac{1}{(2h-2l)!l!}\left(-\frac{Br^2}{k^2\rho'^2_x}\right)^l\\&\times\sum_{h=0}^{n}(-1)^h\binom{n}{n-h}\frac{a^h}{h!}(2h)!(\frac{\mathrm{i}k\rho'_y}{2Br})^{2h}\\&\times\sum_{l=0}^{h}\frac{1}{(2h-2l)!l!}\left(-\frac{Br^2}{k^2\rho'^2_y}\right)^l,\end{aligned} \tag{21}$$

with

$$a=\frac{1}{w_0^2}+\frac{k^2w_0^2}{4r^2}, \tag{22}$$

$$B = \varepsilon + \frac{k^2 w_0^2}{8r^2}. \tag{23}$$

Equation (21) indicates that the average intensity at ($\boldsymbol{\rho}'$, z) depends on beam parameters, such as waist width w_0, beam orders m, n, wavelength λ, turbulence strength $T(\alpha, z)$ including generalized exponent factor α, and the inner and outer scales l_0 and L_0. Equation (21) is applicable to partially coherent scalar nonparaxial H–G beams propagating through non-Kolmogorov turbulence, and is also valid for partially coherent paraxial H–G beams. For $\alpha = 11/3$, $L_0 = \infty$ and $l_0 = 0$, Eq. (21) reduces to the case of the propagation through Kolmogorov turbulence. For $m = n = 0$, Eq. (21) is simplified to the average intensity of GSM beams in non-Kolmogorov turbulence. Specifically, the on-axis average intensity of partially coherent TEM$_{11}$-mode H–G beams in non-Kolmogorov turbulence is expressed as

$$I(0,0,z) = (8kz^2 w_0)^2 \frac{[1/\sigma_0^2 + 2T(\alpha,z)]^2}{[C + 8z^2 T(\alpha,z)]^3}, \tag{24}$$

where

$$C = 4z^2\left(\frac{1}{w_0^2} + \frac{1}{\sigma_0^2}\right) + k^2 w_0^2. \tag{25}$$

Within the framework of paraxial approximation, the average intensity of partially coherent paraxial H–G beams in non-Kolmogorov turbulence can be derived based on the extended Huygens–Fresnel principle[1] and is given by

$$\begin{aligned} &I({\rho'}_x, {\rho'}_y, z) \\ &= \frac{\pi^2 w_0^2}{2\lambda^2 z^2 B'} \exp\left[-\frac{k^2}{4z^2 B'}({\rho'}_x^2 + {\rho'}_y^2)\right] \times 2^{n+m} m! n! \\ &\quad \times \sum_{h=0}^{m} (-1)^h \binom{m}{m-h} \frac{a'^h}{h!} (2h)! \left(\frac{\mathrm{i}k{\rho'}_x}{2B'z}\right)^{2h} \\ &\quad \times \sum_{l=0}^{h} \frac{1}{(2h-2l)!l!} \left(-\frac{B'z^2}{k^2 {\rho'}_x^2}\right)^l \\ &\quad \times \sum_{h=0}^{n} (-1)^h \binom{n}{n-h} \frac{a'^h}{h!} (2h)! \left(\frac{\mathrm{i}k{\rho'}_y}{2B'z}\right)^{2h} \\ &\quad \times \sum_{l=0}^{h} \frac{1}{(2h-2l)!l!} \left(-\frac{B'z^2}{k^2 {\rho'}_y^2}\right)^l, \end{aligned} \tag{26}$$

where

$$a' = \frac{1}{w_0^2} + \frac{k^2 w_0^2}{4z^2}, \tag{27}$$

$$B' = \varepsilon + \frac{k^2 w_0^2}{8z^2}. \tag{28}$$

In numerical calculations, we take partially coherent TEM$_{11}$-mode H–G beams as illustrative examples. The $\lambda = 1.06$ μm, $\sigma_0 = 4$ cm, $\tilde{C}_n^2 = 10^{-14}$ m$^{3-\alpha}$, $L_0 = 1$ m, and $l_0 = 0.001$ m are kept fixed. The evolution of the normalized average intensity distributions $I(\boldsymbol{\rho}', z)/I(\boldsymbol{\rho}', z)_{\max}$ ($I(\boldsymbol{\rho}', z)_{\max}$ is the maximum intensity) of a partially coherent paraxial TEM$_{11}$-mode H–G beam in non-Kolmogorov turbulence with a slanted axis ρ'_r ($\rho'_r = \sqrt{{\rho'}_x^2 + {\rho'}_y^2}$) is plotted in Figs. 1(a) and 1(b) for the generalized exponent factors of $\alpha = 3.5$ and $\alpha = 3.073$, respectively, and $w_0 = 3$ cm. It is shown that for the paraxial case of $w_0 = 3$ cm, Eqs. (26) and (21) deliver the same result, and for our considered partially coherent TEM$_{11}$-mode H–G beams, the paraxial approximation holds true when $w_0 \geq 4\lambda$. From Fig. 1(a), we can see that partially coherent paraxial TEM$_{11}$-mode H–G beams propagating through non-Kolmogorov turbulence undergo several stages of evolution. The average intensity profile has a central dip at plane $z = 0$. At propagation distance $z_{0.5\mathrm{dip}} = 930$ m, the intensity in the centre increases and

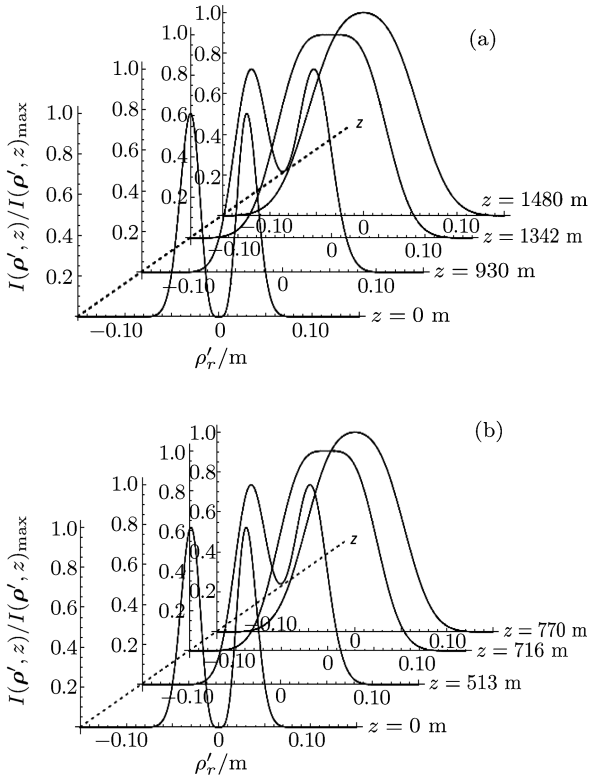


Fig. 1. Evolution of normalized average intensity distributions of partially coherent paraxial TEM$_{11}$-mode H–G beams through non-Kolmogorov turbulence for (a) $\alpha = 3.5$ and (b) $\alpha = 3.073$. The calculation parameters are given in the text.

equals half of the maximum intensity. Furthermore, a flat-topped intensity profile appears at $z_{\mathrm{flat}} = 1342$ m and finally evolves into a Gaussian profile at $z_{\mathrm{Gau}} = 1480$ m. In Fig. 1(b) ($\alpha = 3.073$), the corresponding

evolution distances become $z_{0.5\mathrm{dip}} = 513$ m, $z_{\mathrm{flat}} = 716$ m and $z_{\mathrm{Gau}} = 770$ m. As will be shown in Fig. 4, the turbulence at $\alpha = 3.073$ is stronger than that at $\alpha = 3.5$. Therefore, the evolution behaviour of the average intensity distribution depends on the turbulence and an increase in the turbulence accelerates the evolution process.

Figure 2 shows the evolution of the normalized average intensity distribution of a partially coherent nonparaxial TEM_{11}-mode H–G beam in non-Kolmogorov turbulence with slanted axis ρ'_r. The calculation parameters are $w_0 = 2\lambda$ and $\alpha = 3.5$. As can be seen, the nonparaxial beam hardly changes shape during its propagation through the turbulence. The physical reason is that the diffractive propagation in the free space plays the dominant role for such a case, and the effect of the turbulence is negligible (see Section 3),

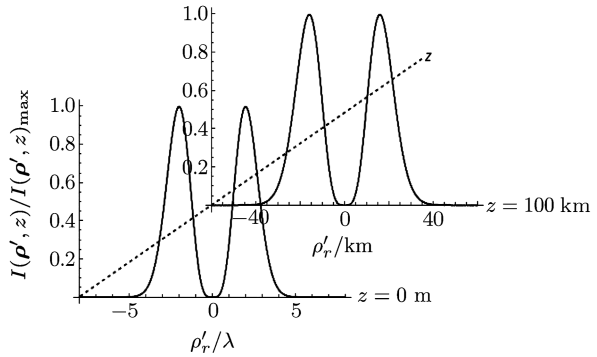


Fig. 2. Evolution of normalized average intensity distribution of the partially coherent nonparaxial TEM_{11}-mode H–G beam through non-Kolmogorov turbulence.

The on-axis average intensity of a partially coherent paraxial TEM_{11}-mode H–G beam in non-Kolmogorov turbulence versus generalized exponent factor α is depicted in Fig. 3 for different propagation distances ($z = 0.5$ km, 1 km and 4 km). The other calculation parameters are the same as those in Fig. 1. It can be seen that, generally, the variation of $I(0, 0, z)$ with α is non-monotonic for the paraxial case and, additionally, it is dependent on the propagation distance z. The results can be interpreted as follows. From Eq. (24), we have

$$\frac{\partial I(0,0,z)}{\partial \alpha} = (16kw_0z^2)^2 \frac{\partial T(\alpha,z)}{\partial \alpha} \frac{[1/\sigma_0^2 + 2T(\alpha,z)]}{[C + 8z^2T(\alpha,z)]^4} \times \left[C - 4z^2T(\alpha,z) - \frac{6z^2}{\sigma_0^2}\right]. \tag{29}$$

Letting $[\partial I(0,0,z)]/\partial\alpha = 0$ leads to

$$\frac{\partial T(\alpha,z)}{\partial \alpha} = 0, \tag{30}$$

or

$$T(\alpha,z) = \frac{1}{w_0^2} - \frac{1}{2\sigma_0^2} + \frac{k^2w_0^2}{4z^2}. \tag{31}$$

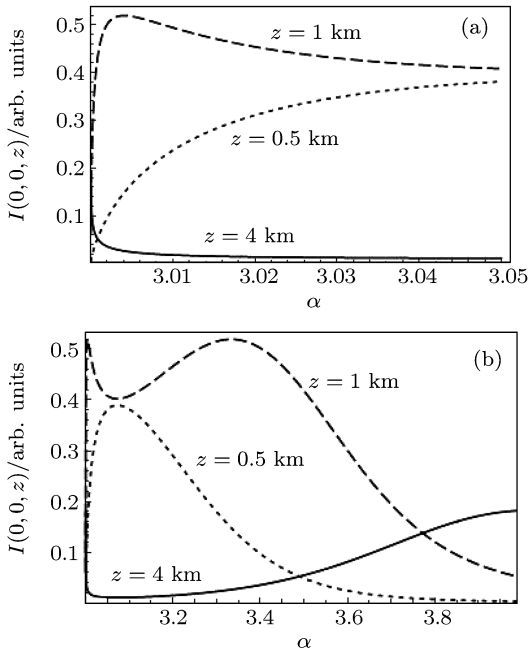


Fig. 3. On-axis intensities of a partially coherent paraxial TEM_{11}-mode H–G beam through non-Kolmogorov turbulence versus generalized exponent factor α at different propagation distances.

The $T(\alpha, z)$ versus α is plotted in Fig. 4 for different propagation distances ($z = 0.5$ km, 1 km, 2 km, and 4 km). Figure 4 shows the non-monotonic behaviour of $T(\alpha, z)$ versus α at a fixed propagation distance z. At $\alpha = 3.073$, $T(\alpha, z)$ reaches its maximum $T(\alpha, z)_{\max}$ determined by $[\partial T(\alpha, z)]/\partial\alpha = 0$, which is independent of z. In the region $3 < \alpha < 3.073$, $T(\alpha, z)$ increases as α increases, while $T(\alpha, z)$ decreases with the α increasing in the region $3.073 < \alpha < 4$. The larger $T(\alpha, z)$ means the stronger turbulence. For $w_0 = 3$ cm at $z = 0.5$ km Fig. 4 indicates that Eq. (31) has no solution. From Eq. (30), we obtain that there exists a maximum for $I(0, 0, 0.5\,\mathrm{km})$, which is achieved at $\alpha = 3.073$. At propagation distance $z = 1$ km, the maximum $T(\alpha, z)_{\max}$ at $\alpha = 3.073$ corresponds to the minimum of $I(0, 0, 1$ km). In addition, it follows from Eq. (31) and Fig. 4 that there are two maxima for $I(0, 0, 1$ km) located at $\alpha = 3.004$ and $\alpha = 3.334$, respectively. At propagation distance $z = 4$ km, Eq. (31) has no solution, and Eq. (30) points out that $I(0, 0, 4$ km) takes its minimum at

$\alpha = 3.073$.

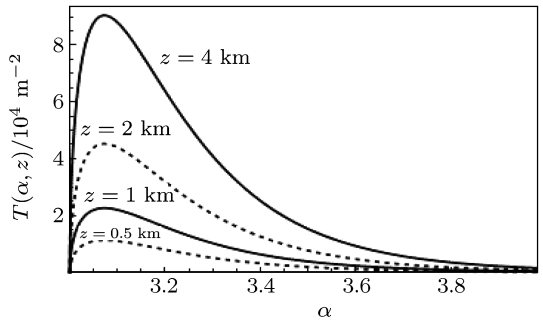


Fig. 4. The $T(\alpha, z)$ versus α at different propagation distances.

Figure 5 shows the variation of $I(0, 0, z)$ with α for a partially coherent nonparaxial TEM_{11}-mode H–G beam through non-Kolmogorov turbulence at different propagation distances ($z = 0.5$ km and 4 km). The other calculation parameters are the same as those in Fig. 2. As can be seen, $I(0, 0, z)$ shows similar variation behaviour with α at different propagation distances for the non-paraxial case, because as shown in Fig. 4 that $T(\alpha, z)$ does not satisfy Eq. (31) for such a case and there exists only one maximum for $I(0, 0, z)$ at $\alpha = 3.073$ determined by Eq. (30).

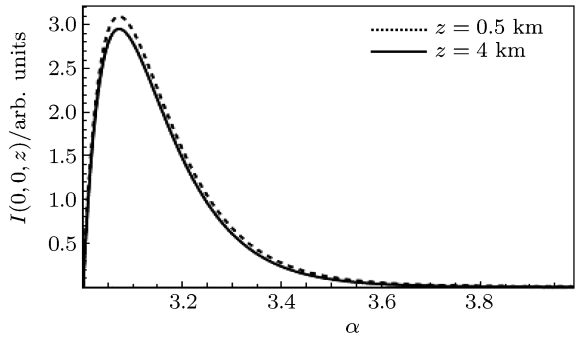


Fig. 5. On-axis intensities of a partially coherent nonparaxial TEM_{11}-mode H–G beam through non-Kolmogorov turbulence versus generalized exponent factor α at different propagation distances.

3. Beam-width spreading of partially coherent H–G beams in non-Kolmogorov turbulence

The root mean squared (RMS) beam width is defined as[10]

$$w(z) = \sqrt{\frac{\iint \rho'^2 I(\boldsymbol{\rho}', z)\mathrm{d}^2\rho'}{\iint I(\boldsymbol{\rho}', z)\mathrm{d}^2\rho'}} = \sqrt{\frac{w_1}{w_2}}, \qquad (32)$$

where

$$w_2 = \pi w_0^2 2^{n+m-1} m!n!. \qquad (33)$$

For the nonparaxial case, a general analytical expression for w_1 could not be found. However, for the paraxial case, the substitution of Eq. (26) into Eq. (32) yields

$$\begin{aligned} w(z) = & \left\{(m+n+1)\frac{w_0^2}{2} + \frac{2z^2}{k^2}\right. \\ & \times \left[(m+n+1)\frac{1}{w_0^2} + \frac{1}{\sigma_0^2}\right] \\ & \left. + \frac{4z^2}{k^2}T(\alpha, z)\right\}^{1/2} \\ = & (\mathrm{I} + \mathrm{II} + \mathrm{III})^{1/2}. \end{aligned} \qquad (34)$$

Equation (34) contains three terms on the right-hand side. The first two terms, I and II, under the square root on the right-hand side represent the diffractive beam-width spreading in free space. The first term is independent of propagation distance z, nd increases with the increases of waist width w_0 and beam orders m, n. The second term is proportional to z^2 and decreases with the increases of w_0 and σ_0 and the decreases of m and n. The third term, III, which is proportional to z^3, describes the spreading due to non-Kolmogorov turbulence. It is readily seen that the larger $T(\alpha, z)$, namely, the stronger turbulence, will result in the larger beam-width spreading.

As shown in Ref. [11], the relative beam width can be introduced to quantitatively describe the resistance of a beam to non-Kolmogorov turbulence and is defined as the ratio of the beam width $w(z)_{\mathrm{turb}}$ of a partially coherent beam in non-Kolmogorov turbulence to the beam width $w(z)_{\mathrm{free}}$ of the same beam in free space ($T(\alpha, z) = 0$). The smaller relative beam width means the reduced influence of the turbulence on the beam-width spreading. From Eq. (34) we obtain

$$w(z)_{\mathrm{turb}}/w(z)_{\mathrm{free}} = [1 + \mathrm{III}/(\mathrm{I} + \mathrm{II})]^{1/2}. \qquad (35)$$

The beam width in turbulence $w(z)_{\mathrm{turb}}$, the beam width in free space $w(z)_{\mathrm{free}}$ and the relative width $w(z)_{\mathrm{turb}}/w(z)_{\mathrm{free}}$ of partially coherent paraxial TEM_{11}-mode H–G beams versus waist width w_0 are plotted in Figs. 6(a) and 6(b) for different propagation distances ($z = 5$ km and 30 km), respectively. The other calculation parameters are the same as those in Fig. 1. Figure 6(a) indicates that $w(z)_{\mathrm{turb}}$ and $w(z)_{\mathrm{free}}$ decrease and $w(z)_{\mathrm{turb}}/w(z)_{\mathrm{free}}$ increases as w_0 increases in the region of $w_0 \in$[1 cm, 4.10 cm). In the region of $w_0 \in$(4.10 cm, 6 cm], $w(z)_{\mathrm{turb}}$ and $w(z)_{\mathrm{free}}$ increase and $w(z)_{\mathrm{turb}}/w(z)_{\mathrm{free}}$ decreases as w_0 increases.

The results can be explained by using Eqs. (34) and (35). From Eq. (34) and $\partial w(z)/\partial w_0 = 0$, we see that the minimum of the beam width is achieved when $w_0 = \sqrt[4]{4z^2/k^2} = w_{0,\min}$. The first term I is smaller than the second term II for $w_0 < w_{0,\,\min}$ and is larger than the second term II for $w_0 > w_{0,\min}$. The first term I is equal to the second term II for $w = w_{0,\min}$. Additionally, the third term III is independent of w_0. At $z = 5$ km in Fig. 6(a), $w_{0,\,\min} = 4.10$ cm From Eqs. (34) and (35), it turns out that the first term I is smaller than the second term II in the region of $w_0 \in$[1 cm, 4.10 cm), thus, the second term II plays the dominant role and $w(z)_{\rm turb}$ and $w(z)_{\rm free}$ decrease and $w(z)_{\rm turb}/w(z)_{\rm free}$ increases with the w_0 increasing. The minima of $w(z)_{\rm turb}$ and $w(z)_{\rm free}$ and the maximum of $w(z)_{\rm turb}/w(z)_{\rm free}$ are achieved at $w_0 = w_{0,\min} = 4.10$ cm. In the region of $w_0 \in$(4.10 cm, 6 cm], the first term I is larger than the second term

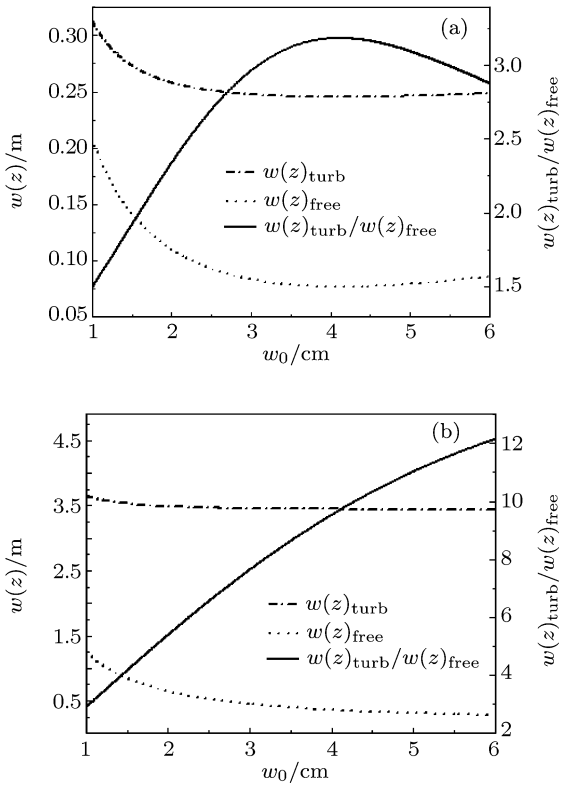


Fig. 6. Beam widths $w(z)_{\rm turb}$, $w(z)_{\rm free}$ and relative width $w(z)_{\rm turb}/w(z)_{\rm free}$ of partially coherent paraxial $\rm TEM_{11}$-mode H–G beams through non-Kolmogorov turbulence versus waist width w_0 at different propagation distances: (a) $z = 5$ km, (b) $z = 30$ km.

II. As a result, $w(z)_{\rm turb}$ and $w(z)_{\rm free}$ increase and $w(z)_{\rm turb}/w(z)_{\rm free}$ decreases with the w_0 increasing.

Furthermore, it can be shown that at a sufficiently long propagation distance, for example, at $z = 30$ km in Fig. 6(b), the third term III will dominate the beam-width spreading, i.e, the third term III is much larger than the sum of the first and the second terms, thus the influence of w_0 on the beam width $w(z)_{\rm turb}$ can be neglected and $w(z)_{\rm turb}$ is nearly independent of w_0. In addition, for such a case, $w_{0,\min} = 10.06$ cm. In the region [1 cm, 6 cm], $w_0 < w_{0,\,\min}$ and the first term I is larger than the second term II, so $w(z)_{\rm free}$ decreases and $w(z)_{\rm turb}/w(z)_{\rm free}$ increases with the w_0 increasing.

Figure 7 shows the beam widths $w(z)_{\rm turb}$ and $w(z)_{\rm free}$ and the relative width $w(z)_{\rm turb}/w(z)_{\rm free}$ of the partially coherent $\rm TEM_{11}$-mode H–G beams at $z = 5$ km versus w_0/λ. The other calculation parameters are the same as those in Fig. 1. It can be seen that for small values of w_0, $w(z)_{\rm turb}$ and $w(z)_{\rm free}$ are not distinguishable, and $w(z)_{\rm turb}/w(z)_{\rm free}$ is hardly dependent on w_0/λ, as shown in Fig. 7. It means that for the non-paraxial case with $w_0 < 4\lambda$ and small values of w_0 as shown in Fig. 7, the diffractive beam-width spreading in free space plays the dominant role, and the effect of the turbulence on the spreading is negligible. In particular, the beam widths $w(z)_{\rm turb}$ and $w(z)_{\rm free}$ increase remarkably and become very large with w_0 decreasing for the non-paraxial case with $w_0 < 4\lambda$.

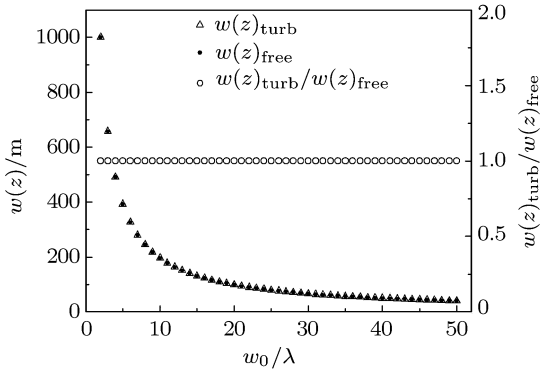


Fig. 7. Beam widths $w(z)_{\rm turb}$, $w(z)_{\rm free}$ and relative width $w(z)_{\rm turb}/w(z)_{\rm free}$ of the partially coherent $\rm TEM_{11}$-mode H–G beams through non-Kolmogorov turbulence at $z = 5$ km versus waist width w_0.

The relative width $w(z)_{\rm turb}/w(z)_{\rm free}$ of the partially coherent paraxial $\rm TEM_{11}$-mode H–G beam versus α is plotted in Fig. 8 for different propagation distances ($z = 0.5$ km, 2 km and 4 km). The other calculation parameters are the same as those in Fig. 1. Figure 8 implies that relative width $w(z)_{\rm turb}/w(z)_{\rm free}$ depends on generalized exponent factor α and propagation distance z for the paraxial case. At $z = 0.5$ km, the diffractive effect dominates the beam-width spreading, so the relative width

$w(z)_{\rm turb}/w(z)_{\rm free}$ is nearly independent of the turbulence strength. With the gradual increase of the propagation distance, say, $z = 2$ km and 4 km, the effect of the turbulence becomes obvious, $w(z)_{\rm turb}/w(z)_{\rm free}$ varies non-monotonically with α and the maximum $w(z)_{\rm turb}/w(z)_{\rm free}$ is achieved at $\alpha = 3.073$. The result can be understood by using Eq. (35) and Fig. 4. Turbulence strength $T(\alpha, z)$ increases with α increasing in the region of $\alpha \in$(3, 3.073) and reaches its maximum at $\alpha = 3.073$, then decreases with α increasing in the region of $\alpha \in$(3.073, 4). Therefore, at $z = 2$ km and 4 km, the values of $w(z)_{\rm turb}/w(z)_{\rm free}$ vary with α in a similar way to that of $T(\alpha, z)$, because for such a case the third term III in Eq. (35) dominates the beam-width spreading.

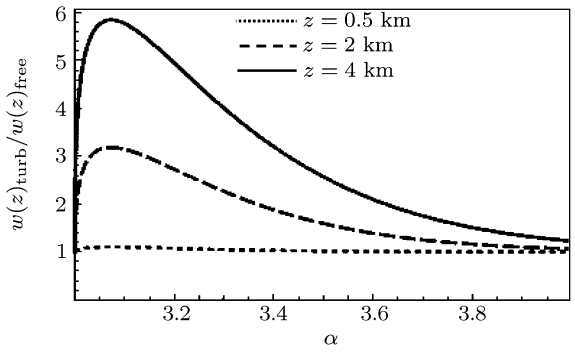


Fig. 8. Relative width $w(z)_{\rm turb}/w(z)_{\rm free}$ of a partially coherent paraxial $\rm TEM_{11}$-mode H–G beam through non-Kolmogorov turbulence versus generalized exponent factor α at different propagation distances.

The relative width $w(z)_{\rm turb}/w(z)_{\rm free}$ of the partially coherent nonparaxial $\rm TEM_{11}$-mode H–G beam versus α are depicted in Fig. 9 for different propagation distances ($z = 0.5$ km and 4 km). The other calculation parameters are the same as those in Fig. 2. From Fig. 9, we see that $w(z)_{\rm turb}/w(z)_{\rm free} = 1$ at $z = 0.5$ km and 4 km. It means that the effect of the turbulence on the beam-width spreading is negligible for the non-paraxial case, which is consistent with the result in Fig. 7. In fact, for any substantial original beam, the beam-width spreading of the partially coherent beams in free space reduces the influence of the turbulence, and for the very large original beam, the beam-width spreading of the partially coherent beams in free space for the non-paraxial case greatly reduces the effect of the turbulence.

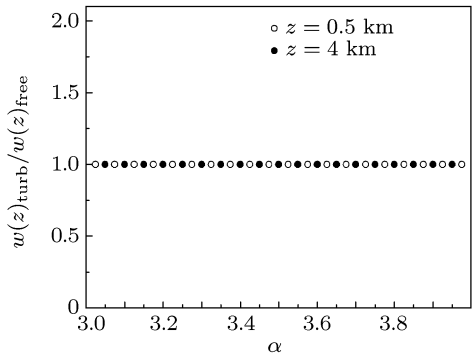


Fig. 9. Relative width $w(z)_{\rm turb}/w(z)_{\rm free}$ of a partially coherent nonparaxial $\rm TEM_{11}$-mode H–G beam through non-Kolmogorov turbulence versus generalized exponent factor α at different propagation distances.

4. Conclusion

In this paper, based on the extended Huygens–Fresnel principle, the propagation properties of partially coherent H–G beams through non-Kolmogorov turbulence are studied analytically and numerically. The effects of the non-Kolmogorov turbulence and beam nonparaxiality on the average intensity evolution and the beam-width spreading are discussed. It is found that the evolution of the average intensity distributions of the partially coherent paraxial H–G beams depends on generalized exponent factor α, namely, on turbulence strength $T(\alpha, z)$. The larger the turbulence strength $T(\alpha, z)$ is, the faster the average intensity evolves for the paraxial case, whereas the beams hardly change shape during their propagation through the turbulence for the non-paraxial case. Depending on waist width w_0 and generalized exponent factor α, the relative widths of the partially coherent H–G beams at different propagation distances vary in different ways for the paraxial case. For the non-paraxial case, the effect of the turbulence is negligible, while the beam-width spreading becomes very large. The results are interpreted by using the analytical expressions derived in this paper and the property of the non-Kolmogorov turbulence. The results obtained in this paper would be useful for understanding the propagation properties of the partially coherent paraxial and non-paraxial beams through the non-Kolmogorov turbulence and for their potential applications, such as parameter optimization in optical communications.[3,28]

References

[1] Andrews L C and Phillips R L 1998 *Laser Beam Propagation Through Random Media* (Bellingham: SPIE)

[2] Young C Y, Gilchrest Y V and Macon B R 2002 *Opt. Eng.* **41** 1097

[3] Korotkova O, Andrews L C and Phillips R L 2004 *Opt. Eng.* **43** 330

[4] Eyyuboğlu H T and Baykal Y 2005 *Appl. Opt.* **44** 976

[5] Eyyuboğlu H T 2005 *Opt. Commun.* **245** 37

[6] Li J, Yang A and Lü B 2008 *J. Opt. Soc. Am.* A **25** 2670

[7] Ji X, Chen X and Lü B 2008 *J. Opt. Soc. Am.* A **25** 21

[8] Yuan Y, Cai Y, Qu J, Eyyuboğlu H T and Baykal Y 2009 *Opt. Express* **17** 11130

[9] Wu J 1990 *J. Mod. Opt.* **37** 671

[10] Gbur G and Wolf E 2002 *J. Opt. Soc. Am.* A **19** 1592

[11] Salem M, Shirai T, Dogarin A and Wolf E 2003 *Opt. Commun.* **216** 261

[12] Shirai T, Dogariu A and Wolf E 2003 *J. Opt. Soc. Am.* A **20** 1094

[13] Chen X, Tang M and Ji X 2008 *Acta Phys. Sin.* **57** 2607 (in Chinese)

[14] Li J, Yang A and Lü B 2009 *Acta Phys. Sin.* **58** 674 (in Chinese)

[15] Stribling B E, Welsh B M and Roggemann M C 1995 *Proc. SPIE* **2471** 181

[16] Be1enkii M S, Karis S J, Brown II J M and Fugate R Q 2010 *Proc. SPIE* **3126** 113

[17] Beland R R 2010 *Proc. SPIE* **2375** 6

[18] Toselli I, Andrews L C, Phillips R L and Ferreroa V 2007 *Proc. SPIE* **6551** 65510E

[19] Toselli I, Andrews L C, Phillips R L and Ferreroa V 2008 *Opt. Eng.* **47** 026003

[20] Wu G, Guo H, Yu S and Luo B 2010 *Opt. Lett.* **35** 715

[21] Chu X, Qiao C and Feng X 2010 *Opt. Commun.* **283** 3398

[22] Siegman A E 1986 *Lasers* (Mill Valley: University Science Books)

[23] Zahid M and Zubairy M S 1989 *Opt. Commun.* **70** 361

[24] Li J, Lü B and Zhu S 2009 *Opt. Express* **17** 11399

[25] Ciattoni A, Corsignani B and Poort P D 2002 *Opt. Commun.* **202** 17

[26] Lü B and Duan K 2003 *Opt. Lett.* **28** 2440

[27] Gradshteyn I S and Ryzhik I M 2007 *Table of Integrals Series and Products* (New York: Academic Press)

[28] Borah D K and Voelz D G 2010 *Opt. Express* **18** 20746